Characterization of Ag+ toxicity on living fibroblast cells by the ferrocenemethanol and oxygen response with the scanning electrochemical microscope

Dongping Zhan, Xiao Li, Alexander B. Nepomnyashchii, Mario A. Alpuche-Aviles, Fu-Ren F. Fan, Allen J. Bard *

Department of Chemistry and Biochemistry, University of Texas at Austin, 1 University Station A5300, Austin, TX 78712-0165, United States

ARTICLE INFO

ABSTRACT

The viability of living fibroblast cells cultured on a Petri dish was determined by scanning electrochemical microscopy (SECM). Three kinds of feedback modes for single living cells were derived with different redox couples: positive, negative and consumptive. The consumptive feedback was unique and distinguished uptake from the response caused by cell deformation. The toxicity of Ag^+ ion on the living fibroblast cells was investigated by using both ferrocenemethanol (FcMeOH) and oxygen (O_2) as electrochemical mediators. The results showed that Ag^+ ions could be taken up and then reduced to form sub-micrometer and micrometer sized metal silver particles. The metal silver particles stained fibroblast cells and give a positive feedback with FcMeOH. These were also identified by the results of both SECM and energy dispersive X-ray spectroscopy (EDX). The amount of consumption of dissolved O_2 decreased with time, showing the cell status as the cells died. Since O_2 is directly involved in cell metabolism and the products of O_2 reduction are not re-oxidized by metal silver particles trapped on fibroblast cells, it is a good SECM mediator to characterize drug effects on cell viability. The results suggest the importance of choice of redox mediator in characterizing cell viability.

1. Introduction

Scanning electrochemical microscopy (SECM) [1] has been used for studies of living cells, e.g., to characterize the viability of living cells (down to the single cell level) and to screen drug effects [2–4]. The photosynthesis of several kinds of plant leaf cells [5–7] and the respiration of a variety of living mammalian cells [8–11] were studied by SECM by detecting changes in the oxygen concentration near the cells. When exposed to cyanide, mammalian cells lose the ability to respire and eventually die because of the binding of cyanide to cytochrome oxidase. These kinds of studies demonstrate that SECM is useful in chemical imaging of cell status in different environments and provides a novel in situ method to screen the effects of drug delivery. Another way to characterize the cell viability by SECM is based on the cellular redox reactions and measurements of mediator turnover [12–17]. The reactivity between cellular redox couples and added mediators depends on the properties of the cell membrane. Generally, hydrophobic mediators give positive feedback since they can permeate the hydrophobic cell membrane. Membrane transports across a living cell or nucleus membrane have also been investigated by the cell-generation/tip-collection mode of SECM [18–20]. The cells take up drug molecules (e.g., menadione) and pump out metabolic products (e.g., thiodione), which can be detected with an SECM tip at μm-distance above the cell. In addition to studies in the constant height mode mentioned above, several groups have also developed a constant distance imaging mode [21,22]. The constant distance mode can overcome the effects caused by the tip-cell interactions, e.g., cell deformation, and has the potential for mapping active sites on the cell membrane.

Silver and its compounds have been used for centuries because of its antibacterial properties [23]. The interactions between different silver containing compounds and bacterial cells have been extensively studied and reviewed [24–26]. Although the exact modes of silver toxicity are still obscure, Ag^+ ion has been proposed to complex with electron donor groups containing sulfur, oxygen or nitrogen, which exist in the bacterial cell in enzymes, polypeptides, proteins, and nucleic acids [27–30]. The normal functions of these cellular components are disrupted and the bacteria eventually die. Silver resistance of bacterial cells has also received much attention from biologists and a silver-binding gene has been identified [31–33]. The silver resistance results from a protective mechanism that pumps the Ag^+ from the cell or from chelation by metal-binding proteins with cysteine or histidine residues [34,35]. The results of Ag^+ uptake and resistance depend on the binding mechanism of Ag^+ in bacterial cells. SECM studies about the Ag^+ effect on the respiratory chain of E. coli suggested that 60% of Ag^+ ion is

* Corresponding author. Tel.: +1 512 471 3761; fax: +1 512 471 0088.
E-mail address: ajbard@mail.utexas.edu (A.J. Bard).

transported within the cell while 40% binds to the outer membrane of the bacterium [36]. More recently, an Ag^+ ion selective SECM tip based on ITIES (the interface between two immiscible electrolyte solutions) was employed to monitor the silver uptake and efflux in situ, and SECM images of fibroblast cells were also obtained [37].

Since antibacterial products containing Ag are used to treat wounds and burns, it is essential to investigate their toxicity on mammalian epithelial tissues [38,39]. When human dermal fibroblast cells were exposed to $AgNO_3$ at concentrations of 4, 12, 82.4 mM for 8 and 24 h, the silver ions greatly inhibited fibroblast proliferation and produced Ag-dependent cell loss. The inhibitory action on DNA synthesis was the primary event in $AgNO_3$ cytotoxicity, associated with significant loss of cell protein. The parallel study of DNA synthesis and cell protein content suggests that the toxic damage produced by silver in different phases of the cell cycle may lead to destruction of the entire cell population and therefore hinder the tissue regeneration process. Ag also causes a concentration- and time-dependent depletion of intracellular ATP content. While the in vitro methods give time-staged changes of certain components, it is useful to use SECM to explore Ag^+ toxicity in real time. The previous study in our group on silver toxicity showed HeLa cells have a strong silver-resistance [17]. In this paper, we study the Ag^+ toxicity on single living fibroblast cells. We propose a new toxicity mechanism derived from the recovered positive SECM feedback by using FcMeOH as redox mediator. The Ag^+ effect on cell viability of fibroblast cells was evaluated from cell respiration determined through monitoring oxygen concentration in the vicinity of cells.

2. Experimental

2.1. Chemicals and materials

$AgNO_3$, $NaNO_3$, KNO_3, $Mg(NO_3)_2$, Ag_2SO_4, Na_2SO_4, K_2SO_4, $MgSO_4$, $NaBH_4$, HEPES, D-glucose were obtained from Fisher. Since Ag^+ ion was present in experimental solutions, halide-free media were used to avoid Ag^+ precipitation: (1) sulfate culture medium contains 1 mM $MgSO_4$, 75 mM Na_2SO_4, 3 mM K_2SO_4, 10 mM glucose, 10 mM HEPES and (2) nitrate culture medium contains 1 mM $Mg(NO_3)_2$, 150 mM $NaNO_3$, 6 mM KNO_3, 10 mM glucose, 10 mM HEPES. All chemicals were reagent grade and used as received. All the aqueous solutions were prepared with deionized water (18 MΩ cm, Milli-Q, Millipore Corp., Billerica, MA).

Dulbecco's modified Eagle's Medium with l-glutamine (DMEM), fetal bovine serum, dimethylsulfoxide (DMSO) and Trypan Blue were provided by the American Type Culture Collection, ATCC (Manassas, VA). Trypsin–EDTA solution was purchased from MP Biomedicals, LLC. HEPES buffered saline solution, and trypsin-neutralizing solution were obtained from Cambrex. All these solutions were used as received.

2.2. Cell culture and experimental preparation

The 3T3 MEFs WT fibroblast cells (CRL-2752™, *Mus musculus* from mouse embryo) were purchased from ATCC and then subcultured in our lab. Cells were grown and maintained in DMEM containing 10% heat-inactivated fetal bovine serum while adhering to the bottom of the Petri dish. The temperature was maintained at 37.5 °C in a water-jacketed incubator (model 2310, VWR Scientific) with 5% CO_2. Cell status and coverage were observed with an inverse optical microscope (Olympus Co., Japan). The cell coverage was controlled to 80 ± 10 % to improve SECM image quality.

Before experiments, the serum-containing DMEM was discarded and the dish was rinsed several times with nitrate medium to remove the growth medium. Then 2 mL of the nitrate culture medium containing 50 μM $AgNO_3$ was added to the Petri dish. After that the cells were incubated for 30 min and rinsed several times with nitrate culture medium again to remove resident Ag^+. Since nitrate is involved in cell metabolism, a sulfate culture medium with 1 mM redox mediator was used during the long time of SECM measurements. To detect oxygen concentration in the vicinity of fibroblast cells, no special manipulation was done and the faradic current resulted from oxygen dissolved in the culture medium from air.

The procedures of cell subculture, the evaluation of cell density and viability were performed according to ATCC directions. The cell viability assay with Trypan Blue was used to compare with experimental results obtained with the SECM. All the cell-dealing procedures were carried out in a sterile fume hood (Liberty Co.). And then the experimental dish was moved and fixed on the SECM stage.

2.3. Instrument and measurements

All the electrochemical measurements were performed with a SECM workstation 900B (CH Instruments, Austin, TX). To avoid chloride contamination of the sulfate culture medium, an Ag/Ag_2SO_4 wire was inserted into a glass tube with saturated Na_2SO_4 solution and sealed with a Vycor tip to construct a reference electrode. A well-polished 10 μm diameter platinum ultramicroelectrode (UME) was used as the SECM tip while a platinum wire served as the counter electrode. For oxygen detection, a hemispherical mercury drop was deposited on a 10 μm diameter platinum UME for the SECM tip [40]. On the Hg hemispherical UME, the products of the 2e oxygen reduction are H_2O_2 and OH^-. The faradic current is much more stable than that on a bare Pt tip. A deoxygenated solution of 1.0 M KNO_3 containing 5.7 mM mercurous ion and 0.5% nitric acid was used for mercury deposition. Mercury deposition on platinum microelectrodes was carried out at a constant potential of 0.2 V (vs. Ag wire) for 180 s. Following deposition the electrodes were washed with deionized water and checked with an optical microscope (Olympus Co., Japan) before further use. A SECM image scan was performed to locate a single living cell and the tip was then positioned over it to obtain approach curves. To elucidate the "recovered" positive feedback image obtained by FcMeOH (see below), μm-sized silver metal particles were electrolessly deposited on a glass slide by the reaction between dilute $AgNO_3$ and $NaBH_4$ aqueous solution.

SEM and EDX (Zeiss/LEO, Oberkochen) experiments also were done to elucidate the results obtained by SECM. The procedure for preparation of SEM samples was as follows: The cell suspension with an estimated cell density of 10^6/mL was dropped onto a 20 nm thick gold film, which was deposited on a 1 cm × 1 cm glass slide with a metal evaporator DV 502A (Denton Vacuum, Moorestown, NJ). Cells were allowed to attach to the gold film overnight. Then the cells were rinsed with nitrate culture medium and incubated with 50 μM Ag^+ ions for 30 min. The cells were rinsed with nitrate culture medium several times and incubated in sulfate medium for 24 h. The samples were taken out and rinsed with Milli-Q water carefully several times to remove the salts. Finally the samples were dried in the sterile hood for SEM and EDX experiments.

3. Results and discussion

3.1. SECM feedback on living fibroblast cells

SECM has a unique advantage over other types of scanning probe microscopy (SPM) because it can provide the local chemical activity in the vicinity of living cells. SECM has been shown to be a

useful in situ method to characterize the cell viability and drug effects in recent years [2]. By using suitable redox mediators, three kinds of SECM feedback were found; these are summarized here according to the tip current response obtained on single living cells (shown in Fig. 1a–c): (a) positive feedback, i.e., the mediator is recycled by the living cell and the tip current increases when a tip approaches the cell vertically; (b) negative feedback, i.e., the mediator is not recycled by the living cell and tip current decreases during approach due to the blocking effect of the cells; (c) consumptive or shielding feedback, i.e., the mediator is involved in the cell metabolism and is consumed by the living cell. During the approach the tip and the cell compete for the mediator in the tip-cell gap, which makes the approach curve fall below the negative feedback curve. These feedback modes were observed on the single living fibroblast cells by using different redox mediators. Fig. 1d shows the different feedback found with FcMeOH, $Co(bpy)_3^{2+}$ or O_2 obtained above a single living fibroblast cell. Since the negative feedback reflected only the blocking effect of the cell shape, it could be used as a benchmark (shown as Curve 2 in Fig. 1d). $FcMeOH^+$ generated on the SECM tip could be reduced to FcMeOH by the single living fibroblast cells. Thus, the approach curve for FcMeOH (Curve 1 in Fig. 1d) shows higher currents than Curve 2. Note that the current during a cell approach by the tip does not correspond to the mass transfer controlled positive feedback approach curve in SECM, e.g., as seen with an electroactive substrate. Rather, in this cell approach curve the tip feedback is limited by the kinetics of the redox process on the substrate, i.e., the kinetics of the reduction of $FcMeOH^+$ by the cell [1]. On the contrary, O_2 is involved in the metabolism of single living fibroblast cells that compete for O_2 with the SECM tip. As a result, this is a shielding approach curve that falls below the theoretical negative feedback curve (Curve 3 in Fig. 1d) [41]. These results show that one should consider not only the redox potential of the mediator but also the reactivity of the chosen mediator with cell components. In general, hydrophobic redox mediators sometimes show positive feedback, because they can penetrate the cell membrane, while hydrophilic mediators often show negative feedback [14,17].

It is important to confirm that deviation for the O_2 approach curve (Fig. 1d–3) from negative feedback is caused by O_2 consumption by the cell rather than by cell topography, since both cases can produce a net reduction in tip current as compared to $i_{t,\infty}$, the diffusion limited current of the tip when it is far from the cell. Experiments were done to identify the difference between the two cases and the results were shown in Fig. 2. Fig. 2a shows the difference between the approach curves above single living fibroblast cells with coverage of 85 ± 5 % using $Co(bpy)_3^{2+}$, which generates negative feedback, and O_2 as mediators. Note that the normalized approach curve, $I_T = i_t/i_{t,\infty}$ vs. normalized distance, d/a, of O_2 lies well below that of $Co(bpy)_3^{2+}$. If the living fibroblast cells did not consume oxygen, both normalized approach curves should be the same within experimental error due to the cell shape. Another experiment (Fig. 2b) shows the normalized current, I_T vs. tip displacement for oxygen consumption of living and dead fibroblast cells. The triangle point line is the negative feedback over the bottom of the Petri dish without cells (an insulator). The square point line is the consumptive feedback of oxygen over single living fibroblast cells. The circle point line is the approach curve over fibroblast cells exposed to the experiment medium containing 20 mM sodium cyanide for 30 min. The result of a Trypan Blue experiment showed that most of the cells died after 20 min exposure to 20 mM cyanide. The significant difference between live and dead cells (the latter essentially the same as the negative feedback over the insulator) showed that correspondence between the nature of the feedback and cell viability is good. These results show that the consumptive feedback approach curves depend strongly on the viability of the cells. As living cells gradually lost their viability, the shape of the feedback curves would change finally overlapping with a negative feedback approach curve. Over the time scale of our experiments, the cells maintain their shape as observed with an inverted optical microscope, in agreement with previously reported results [10]. Thus, our results confirm that our definition of consumptive feedback is reasonable.
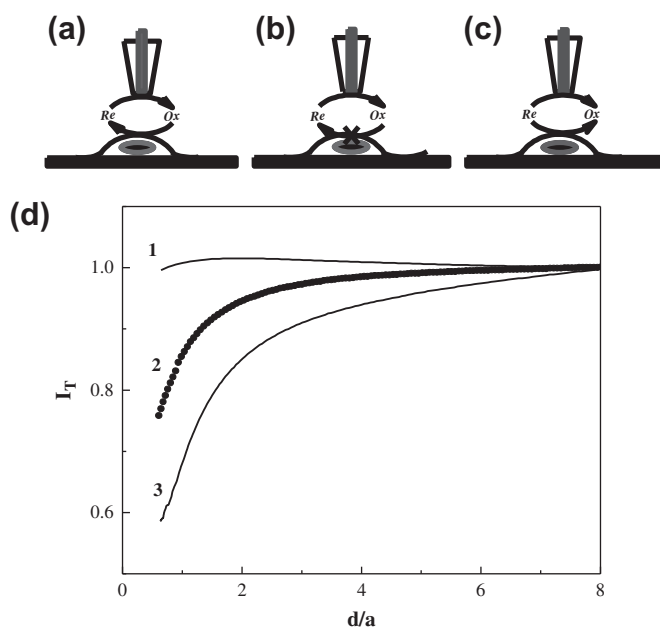
3.2. SECM images based on different feedback modes with living fibroblast cells

One can characterize the viability of living cells with SECM images. The difference between the normal cells and abnormal cells provides information on the cell behavior in various environments, especially for the mechanism of drug delivery and cell metabolism. As discussed above the SECM image is based on differences between negative, positive and consumptive feedback. Usually the SECM tip is placed on a region without living cells and fixed at a certain distance (usually 10–15 μm) above the bottom of a Petri dish through the negative feedback curve with a mediator of choice. Then the SECM tip is moved above a living cell region to obtain the SECM image. Fig. 3 shows the SECM images obtained by a hemispherical Hg tip with FcMeOH (Fig. 3b), $Co(bpy)_3^{2+}$ (e) and O_2 (c and f). FcMeOH shows positive feedback because it is oxidized at the tip and the ferrocenium form can interact with reduced material in the cell. $Co(bpy)_3^{2+}$ on the other hand, shows negative feedback, even though the +3 form is more oxidizing than ferrocenium, presumably because it is too hydrophilic to enter the cell membrane. After the cell image with FcMeOH (b) or $Co(bpy)_3^{2+}$ (e) was obtained, the potential was switched to that for oxygen reduction to obtain an image of the oxygen distribution in the vicinity of the same cells (c and f). In accordance with the feedback of these redox mediators as described above, FcMeOH gave a positive feedback and the current in the vicinity of single living fibroblast cells was higher than the background. The background corresponds to the Petri dish
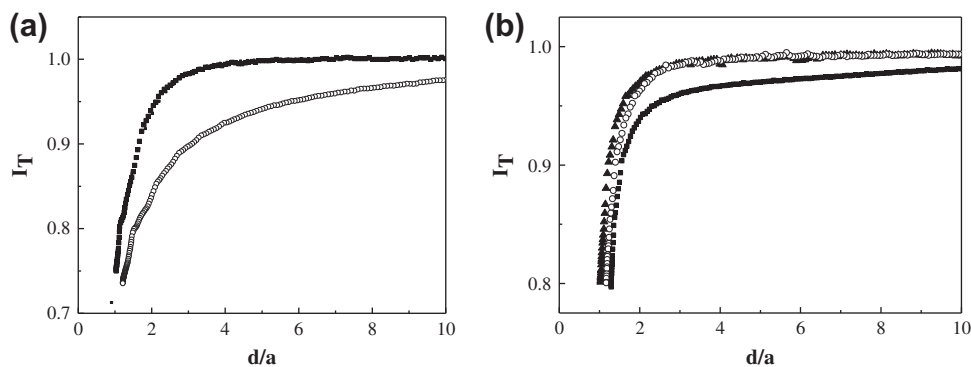

Fig. 1. Schematics (a–c) and approach curves (d) of the feedback modes for single living fibroblast cells. (a) Positive feedback (curve d-1, 1 mM FcMeOH); (b) negative feedback (curve d-2, 1 mM $Co(bpy)_3^{2+}$); (c) consumptive feedback (curve d-3, dissolved O_2 from air, ca. 0.25 mM). Hg/Pt hemispheric tip in sulfate medium, the approach rate is 1 μm/s.

Fig. 2. Approach curve of a Hg/Pt tip over fibroblast cells (a) comparison of (■) $Co(bpy)_3^{2+}$ oxidation and (o) O_2 reduction. (b) O_2 reduction of living fibroblast cells before (■) and after (o) exposure to 20 mM NaCN for 20 min. (▲) O_2 reduction approach curve to a clean Petri dish. All other conditions are the same as shown in Fig. 1.
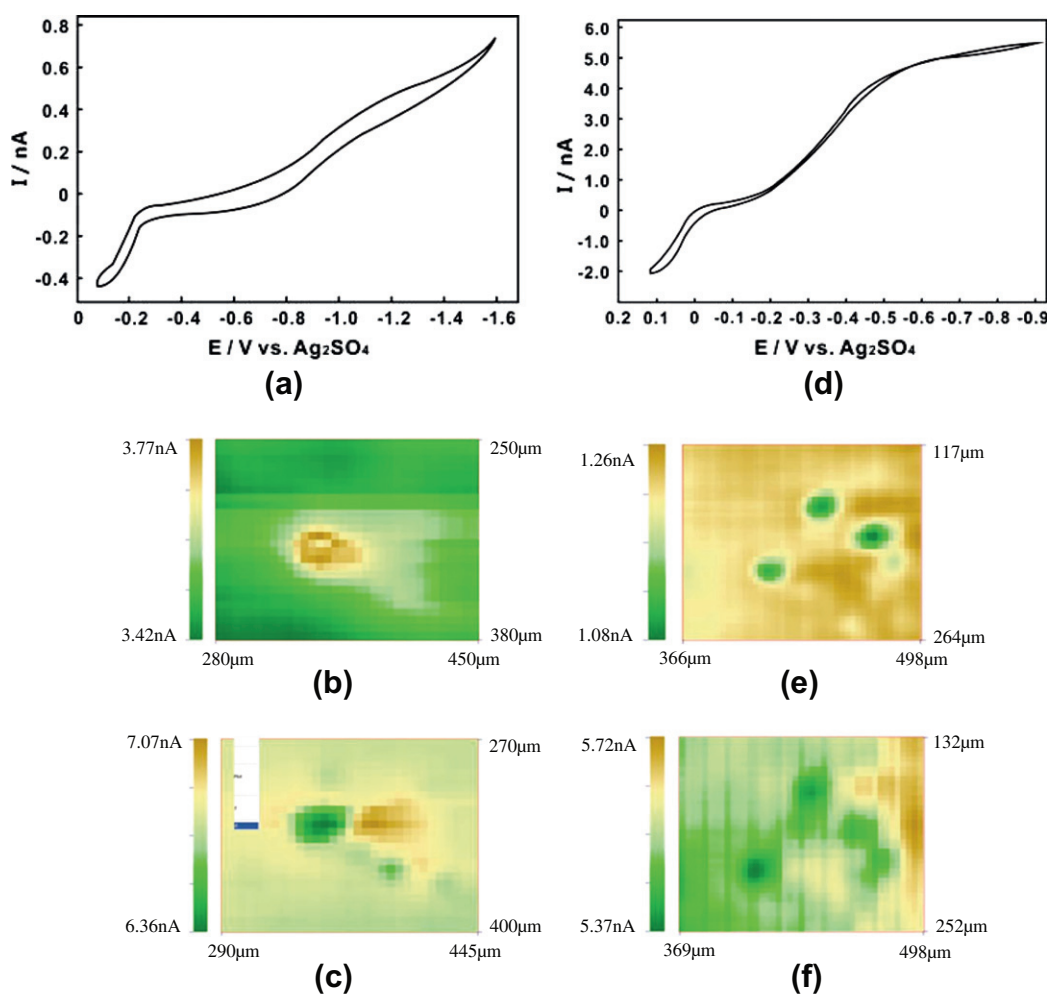

Fig. 3. Comparison of FcMeOH, O_2 and $Co(bpy)_3^{2+}$ imaging results. (a) Cyclic voltammograms (CV) for 1 mM FcMeOH oxidation and O_2 reduction with a scan rate of 50 mV/s, (b and c) SECM images of the same fibroblast cells with (b) FcMeOH at −0.1 V and with (c) O_2 at −1.4 V. (d) CV for $Co(bpy)_3^{2+}$ oxidation and O_2 reduction with a scan rate of 50 mV/s. (e and f) SECM images of the same fibroblast cells with (e) $Co(bpy)_3^{2+}$ at 0.1 V and (f) with O_2 at −0.8 V. The scan rate is 100 μm/s while all other conditions are the same as in Fig. 1.

surface blocking diffusion to the tip, i.e., negative feedback. As to $Co(bpy)_3^{2+}$ and oxygen, the currents in the vicinity of single living fibroblast cells were lower than the background. For $Co(bpy)_3^{2+}$, the contrast comes from the cell hindering diffusion to the tip more efficiently than the surface of the dish, i.e., an effect of the cell shape. For O_2, in addition to the blocking of mass trans-

port to the tip, the tip detects a lower concentration of O_2 because of cell respiration. The image contrast is a function of cell viability, cell shape, diffusion coefficient of the redox mediators and the interaction between the living cells and the mediators. For the same mediator, the image strength depends strongly on the cell viability, which is discussed in the following sections.
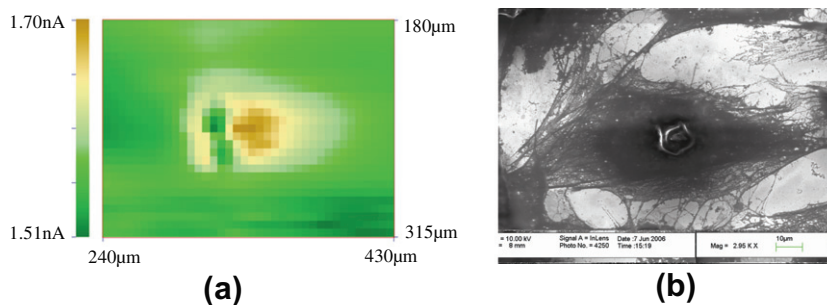
Fig. 4. (a) SECM image of a single living fibroblast cell with a Pt tip in sulfate medium with 1 mM FcMeOH, the tip potential is held at 0.3 V while the scan rate is 100 µm/s. (b) SEM image of a dried fibroblast cell. The SEM accelerator voltage is 10.00 kV and the scale bar is 10 µm.
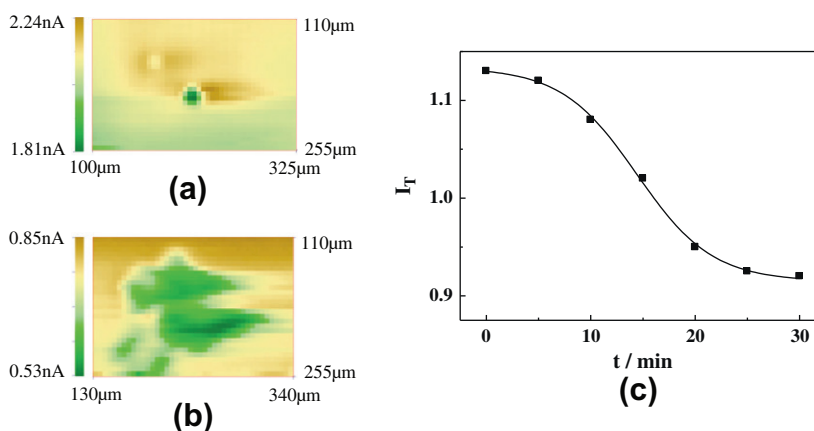

Fig. 5. SECM images (a and b) for cell viability determination. (a) Fibroblast cells (coverage 85%) before and (b) after exposure to 20 mM NaCN for 25 min. Pt tip in sulfate medium with 1 mM FcMeOH, the tip potential is held at 0.3 V while the scan rate is 100 µm/s. (c) Cell viability change with exposure time, the viability was calculated by the average ratio between the tip current above the cell and that above the Petri dish obtained from the cells in a 500 µm × 500 µm region.

3.3. Mechanism of Ag$^+$ ion toxicity characterized by FcMeOH

Single fibroblast cells cultured on the bottom of the Petri dish with a coverage of 85 ± 5 % were used for SECM imaging. The sulfate culture medium containing 1 mM FcMeOH was added into the Petri dish for SECM experiments. A typical image of a single fibroblast cell is shown in Fig. 4a (compared to the SEM image shown in Fig. 4b). The cell size in SECM images agrees with that observed by SEM. Since both the diffusion coefficient ($\sim$7 × 10^{-6} cm^2/s) [41] and the kinetic rate of reduction are relatively large, the FcMeOH$^+$ generated by the tip that diffuse to the cell, enter the membrane and are reduced, giving a relatively weak positive feedback in the ambient membrane region.

Fig. 5 illustrates the difference between normal single living fibroblast cells (a) and dead ones (b), killed with 20 mM cyanide for 25 min. As mentioned above, the results of Trypan Blue essay show that most of the living cells die after this treatment with cyanide. Only living cells give positive feedback while dead cells give negative feedback. This is the basis of determining cell viability by SECM imaging. As the CN$^-$ exposure time increases, the ratio of the current in the cell region to background current changes from the initial positive feedback to a final negative feedback (dead cells). Thus, the viability can be determined from the ratio of the tip current over the cells to that over the Petri dish surface. Fig. 5c shows the static viability change with time after the addition of 20 mM cyanide to the sulfate culture medium with a single fibroblast cell. Cyanide anions are reported to combine with proteins in the respiration chain of fibroblast cells and kill the cell rapidly, so cell respiration ceases. These results agree with previous reports from the Matsue group [10].

Ag$^+$ toxicity was also evaluated by SECM using FcMeOH as redox mediator. The fibroblast cells cultured on the Petri dish (coverage, 85 ± 5%) were rinsed with a nitrate culture medium several times. Then 50 µM AgNO$_3$ was added to the nitrate culture medium and the cells incubated for 30 min. Then the cells were rinsed with nitrate culture medium several times to remove the Ag$^+$ left in the medium. Finally, a sulfate culture medium was added to perform the SECM experiments. The viability of fibroblast cells, as defined by the ratio of tip current over the cells to that over the Petri dish background was studied after addition of 50 µM FcMeOH (Fig. 6d). The viability decreased with time, but at longer times (t > 150 min), the cells continued to maintain a relatively weak positive feedback current that never changed to negative feedback, as expected if all of the cells died. When the cells were kept on the SECM stage overnight, positive feedback recovered. For comparison, Trypan Blue experiments showed that the fibroblast cells, which survived for more than 7 h in a sulfate medium without Ag$^+$, died after about 2 h when exposed to 50 µM Ag$^+$ ions. Fig. 6 shows the first image (a) and the image after 24 h (b) of the same cell. The strength of the positive feedback was enhanced a little after 24 h. This "recovered" positive feedback is caused by production of metallic Ag particles which can act as open circuit metallic substrates; a SECM image with FcMeOH on the silver particles electrolessly deposited on glass is shown in Fig. 6c. Thus the experiment with cells can be explained as: (1) an initial decrease of the feedback strength reflecting loss of cell viability at the first stages after the addition of Ag$^+$ and (2) Ag$^+$ ions taken up by the cells being reduced to Ag metal particles. These particles form up to µm sizes and are immobilized on or inside the cell membrane, so the cells resemble a Ag-particle substrate and show positive
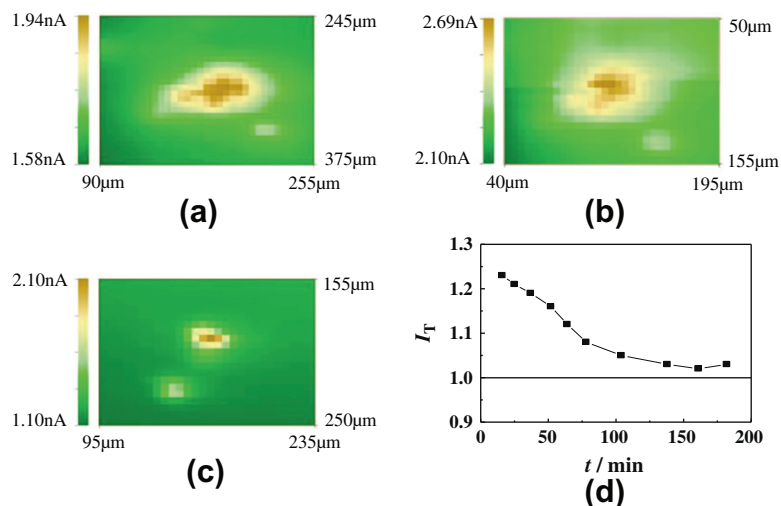
Fig. 6. Cell images of a same fibroblast cell derived from FcMeOH after fibroblast cells were incubated with 50 μM AgNO₃ for 30 min: (a) immediately after incubation and (b) after 24 h. (c) is the image of a metal silver particle electrolessly deposited on a glass slide. (d) The viability change of fibroblast cells with time in 3 h. Tip: 10 μm diameter Pt disk. Solution: sulfate medium with 1 mM FcMeOH. The tip potential is held at 0.3 V while the tip raster rate is 100 μm/s.

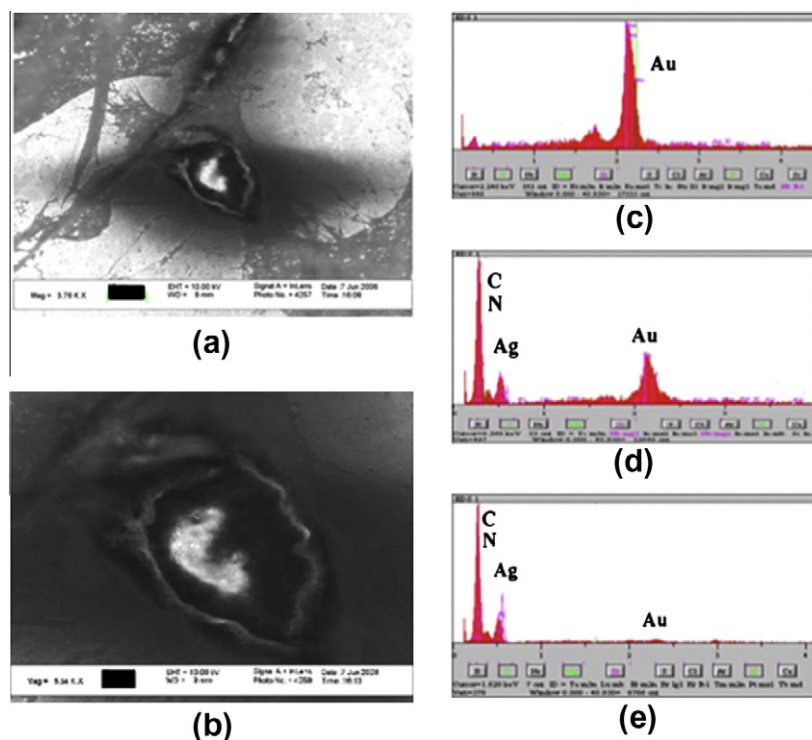**Fig. 7.** SEM studies of a dried fibroblast cell after incubation in nitrate medium with 50 μM AgNO₃ for 30 min: (a) image of the cell, (b) detail of the nucleus. (c–e) EDX analysis: (c) Au/glass slide, (d) cell membrane and (e) nucleus. The SEM accelerator voltage is 10.00 kV and the scale bars are 10 μm (a) and 3 μm (b).

feedback of FcMeOH at open circuit. The fact that these particles have radii of the order or smaller than the radius of the scanning tip disk yet show feedback characteristic of a larger conductive substrate suggests that these particles are somehow interconnected, so that the reduction reaction of the ferrocenium form can be compensated by oxidation of FcMeOH at a location not under the tip.

The formation of Ag particles was also verified by SEM and EDX measurements (Fig. 7). SEM shows a large bright block in the region of the nucleus, which has a higher conductivity than other cell regions (Fig. 7a and b). EDX showed the elements in different re-

gions of the cell (cell membrane Fig. 7d, nucleus 7e) and the background (Au substrate, 7c) and confirm the main element of the bright region is silver. Since Ag⁺ ion is a strong oxidant, it would be reduced by any reductants existing in the cell to form metallic silver particles. Ag particles have been extensively studied as an antibiotic for bacteria, so the particles themselves may be responsible for cell death. The smaller particles can grow and aggregate and thus connect with each other to form larger conductive islands, resulting in the positive feedback that is recovered after 24 h. Thus in studies of heavy metal toxicity using SECM and redox mediators, one must be careful to eliminate feedback from metal
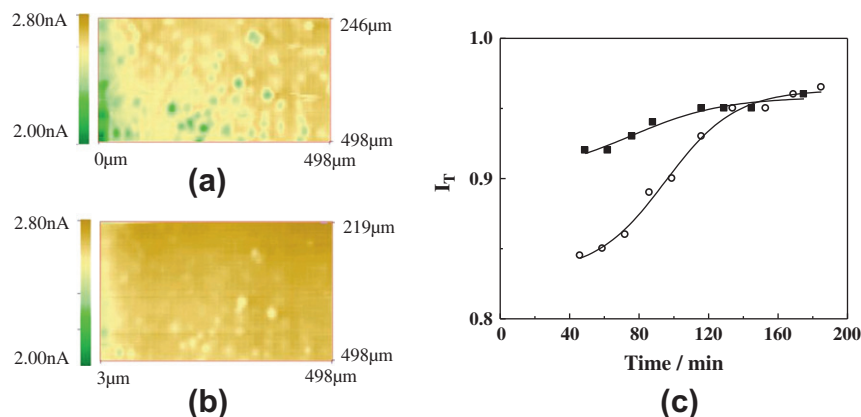
Fig. 8. Oxygen consumption images of living fibroblast cells: (a) before and (b) after 20 min incubation in 20 mM NaCN. Tip potential is −1.2 V while scan rate is 100 μm/s. (c) The viability change of fibroblast cells with time after fibroblast cells were incubated with AgNO₃ for 30 min, the concentration of AgNO₃ are (■) 200 μM and (o) 20 μM. Tip and electrolyte: Hg/Pt hemispheric electrode in sulfate medium.

particles as a measure of cell viability. One must also investigate whether the metabolic products of the drug being studied react with the redox mediator spontaneously.

In summary, although FcMeOH feedback does not give an unambiguous response of single fibroblast cell viability upon exposure to Ag⁺, it can provide time-dependent information about Ag⁺ toxicity, before Ag nanoparticles formation dominates the response.

3.4. SECM characterization of Ag⁺ toxicity by oxygen reduction imaging

An alternative approach to SECM imaging of single fibroblast cell viability is to study its respiration by determining the oxygen concentration above the cell by its reduction at the tip. A hemispherical Hg drop electrode was used as the SECM tip [40]. Fig. 8 shows images of fibroblast cells (a) before and (b) after 20 min exposure to 20 mM CN⁻, shown with the same color scale, where green represents smaller currents and yellow/brown the background oxygen reduction on the Petri dish. Living cells show obvious oxygen consumption above the cells (see Fig. 8a), while after the introduction of NaCN to kill the cells, only background O₂ reduction and thus negative feedback was observed (see Fig. 8b). Results for Ag⁺ are shown in Fig. 8c. Note that the feedback never changed to positive feedback even after 24 h, indicating that the product of oxygen reduction (H₂O₂) was not re-oxidized by Ag particles on the cells. Thus respiration and oxygen detection is a good way to characterize Ag⁺ toxicity. Note here, since the cells consume oxygen and decrease the current, that an increase in the $i_t/i_{t,\infty}$ ratio indicates cell death, opposite to the FcMeOH case. Fig. 8c shows the changes of single fibroblast cells viability with time after the cells were incubated in the sulfate culture medium with different Ag⁺ ion concentrations. An obvious change of cell viability could be observed when incubated in the solution with lower Ag⁺ ion concentration as evident from the slow increase in the $i_t/i_{t,\infty}$ ratio. When the concentration was 200 μM, the viability was very small from the beginning of the SECM scan and there is a smaller change of viability with time. The reported results of MTT and BrdU assays showed that the reproducible Ag⁺ toxic dose on human dermal fibroblast cells ranged from 4.12 to 82.4 μM [38,39]. There might be different mechanisms for silver toxicity for low and high Ag⁺ concentrations. When cells were exposed to the Ag⁺ with the concentration in this range (20 μM), the cell took up Ag⁺ ions fast enough that Ag⁺ ion did not deposit in the cells by chemical interactions with cell components. There are many time-dependent interactions between cell components and Ag⁺ ions, including

redox reactions, association/dissociation, aggregation and cell deformation. These processes would disturb functions of DNA, enzymes, and proteins. As a result, the cells would gradually die and slowly decrease their respiration rate. When the concentration of Ag⁺ is higher than this interval, the Ag⁺ ion can suddenly precipitate on the membrane and block mass transfer and communication between the cells and their environment. In this case the cells showed low viability from the beginning and little changes during the subsequent time. In the clinic, the use of high concentrations of Ag⁺ usually causes black spots on the skin that disappear after several days. This is consistent with the death of skin cells and denaturation of protein caused by sudden deposition of Ag.

4. Conclusions

Three kinds of SECM feedback modes were obtained with single living fibroblast cells: positive, negative and consumptive or shielding, according to the local current response obtained by the SECM tip. The SECM images based on the different feedback modes were verified from approach curves with appropriate redox mediators. Changes in cell viability were followed by SECM imaging. Silver toxicity was investigated by using FcMeOH and oxygen as redox mediators. Since FcMeOH could be recycled by silver metal particles, the cells produced a net positive feedback. The recovering of FcMeOH positive feedback and an ultimate steady-state current indicated that the silver ion taken up by the cells could be reduced and aggregated to form silver metal particles. This unique mechanism was uncovered by in situ SECM and confirmed by SEM and EDX measurements. On the contrary, the whole process of fibroblast cell death could be monitored measuring respiration of dissolved O₂ as the SECM mediator because the products of oxygen reduction are not recycled on silver metal particles formed inside the cells. The silver toxic dose found with SECM agreed with the results of MTT and BrdU methods.

References

[1] A.J. Bard, M.V. Mirkin (Eds.), Scanning Electrochemical Microscopy, second ed., Taylor and Francis, New York, 2012.

[2] J. Mauzeroll, S.B. Schougaard, SECM of living cells, in: A.J. Bard, M.V. Mirkin, (Eds.), Scanning Electrochemical Microscopy, 2nd Ed. Taylor and Francis, New York, 2012, Chapter 12.

[3] A.J. Bard, X. Li, W. Zhan, Chemically imaging living cells by scanning electrochemical microscopy, Biosens. Bioelectron. 22 (2006) 461–472 (and references cited therein).

[4] S. Amemiya, J. Guo, H. Xiong, D.A. Gross, Biological applications of scanning electrochemical microscopy: chemical imaging of single living cells and beyond, Anal. Bioanal. Chem. 386 (2006) 458–471.

[5] C. Lee, J. Kwak, A.J. Bard, Application of scanning electrochemical microscopy to biological samples, Proc. Natl. Acad. Sci. USA 87 (1990) 1740–1743.

[6] M. Tsionsky, Z.G. Cardon, A.J. Bard, R.B. Jackson, Photosynthetic electron transport in single guard cells as measured by scanning electrochemical microscopy, Plant Physiol. 113 (1997) 895–901.

[7] R.K. Zhu, S.M. Macfie, Z.F. Ding Cadmium-induced plant stress investigated by scanning electrochemical microscopy, J. Exp. Bot. 56 (2005) 2831–2838.

[8] T. Yasukawa, T. Kaya, T. Matsue, Characterization and imaging of single cells with scanning electrochemical microscopy, Electroanalysis 12 (2000) 653–659.

[9] T. Yasukawa, Y. Kondo, I. Uchida, T. Matsue, Imaging of cellular activity of single cultured cells by scanning electrochemical microscopy, Chem. Lett. 27 (1998) 767–768.

[10] T. Kaya, Y.S. Torisawa, D. Oyamatsu, M. Nishizawa, T. Matsue, Monitoring the cellular activity of a cultured single cell by scanning electrochemical microscopy (SECM). A comparison with fluorescence viability monitoring, Biosens. Bioelectron. 18 (2003) 1379–1383.

[11] H. Shiku, Y.S. Torisawa, A. Takagi, S. Aoyagi, H. Abe, H. Hoshi, T. Yasukawa, T. Matsue, Metabolic and enzymatic activities of individual cells, spheroids and embryos as a function of the sample size, Sens. Actuators B 108 (2005) 597–602.

[12] M.V. Mirkin, B. Liu, S.A. Rotenberg, Probing redox activity of human breast cells by scanning electrochemical microscopy, Methods Enzymol. 352 (2002) 112–122.

[13] S.A. Rotenberg, M.V. Mirkin, Scanning electrochemical microscopy: detection of human breast cancer cells by redox environment, J. Mammary Gland. Biol. Neoplasia 9 (2004) 375–382.

[14] B. Liu, S.A. Rotenberg, M.V. Mirkin, Scanning electrochemical microscopy of living cells. 4. Mechanistic study of charge transfer reactions in human breast cells, Anal. Chem. 74 (2002) 6340–6348.

[15] Y. Takahashi, T. Miyamoto, H. Shiku, R. Asano, T. Yasukawa, I. Kumagai, T. Matsue, Electrochemical detection of epidermal growth factor receptors on a single living cell surface by scanning electrochemical microscopy, Anal. Chem. 81 (2009) 2785–2790.

[16] T. Yasukawa, I. Uchida, T. Matsue, Dual imaging of topography and photosynthetic activity of a single protoplast by scanning electrochemical microscopy, Biochim. Biophys. Acta 1369 (1998) 152–158.

[17] X. Li, A.J. Bard, Scanning electrochemical microscopy of HeLa cells – effects of ferrocene methanol and silver ion, J. Electroanal. Chem. 628 (2009) 35–42.

[18] J. Mauzeroll, A.J. Bard, Scanning electrochemical microscopy of menadione-glutathione conjugate export from yeast cells, Proc. Natl. Acad. Sci. USA 101 (2004) 7862–7867.

[19] J. Mauzeroll, A.J. Bard, O. Owhadian, T.J. Monks, Menadione metabolism to thiodione in hepatoblastoma by scanning electrochemical microscopy, Proc. Natl. Acad. Sci. USA 101 (2004) 17582–17587.

[20] J. Guo, S. Amemiya, Permeability of the nuclear envelope at isolated Xenopus Oocyte nuclei studied by scanning electrochemical microscopy, Anal. Chem. 77 (2005) 2147–2156.

[21] R.T. Kurulugama, D.O. Wipf, S.A. Takacs, S. Pongmayteegul, P.A. Garris, J.E. Baur, Scanning electrochemical microscopy of model neurons: constant distance imaging, Anal. Chem. 77 (2005) 1111–1117.

[22] A. Hengstenberg, A. Blöchl, I.D. Dietzel, W. Schuhmann, Spatially resolved detection of neurotransmitter secretion from individual cells by means of scanning electrochemical microscopy, Angew. Chem. Int. Ed. Engl. 40 (2001) 905–908.

[23] N. Grier, Silver and its compounds, in: S. Seymour (Ed.), Disinfection, Sterilization, and Preservation, secon ed., Lea & Febiger, Philadelphia, PA, 1977, pp. 395–407.

[24] A.D. Russell, W.B. Hugo, Antibacterial action and activity of silver, Prog. Med. Chem. 31 (1994) 351–371.

[25] G. Schultz, R.G. Sibbald, V. Falanga, A. Ayello, C. Dowsett, K. Harding, M. Romanelli, M. Stacey, L. Teot, W. Vanscheidt, Wound bed preparation: a systematic approach to wound management, Wound Repair Regen. 11 (2003) 1–28.

[26] J.T. Trevors, Silver resistance and accumulation in bacteria, Enzym. Microb. Technol. 9 (1987) 331–333.

[27] W.J. Schreurs, H. Rosenberg, Effect of silver ions on transport and retention of phosphate by Escherichia coli, J. Bacteriol. 152 (1982) 7–13.

[28] P. Dibrov, J. Dzioba, K.K. Gosink, C.C. Hase, Chemiosmotic mechanism of antimicrobial activity of Ag^+ in Vibrio cholerae, Antimicrob. Agents Chemother. 46 (2002) 2668–2670.

[29] Q.L. Feng, J. Wu, G.Q. Chen, F.Z. Cui, T.N. Kim, J.O. Kim, A mechanistic study of the antibacterial effect of silver ions on Escherichia coli and Staphylococcus aureus, J. Biomed. Mater. Res. 52 (2000) 662–668.

[30] L. Zeiri, B.V. Bronk, Y. Shabtai, J. Eichler, S. Efrima, Surface-enhanced Raman spectroscopy as a tool for probing specific biochemical components in bacteria, Appl. Spectr. 58 (2004) 33–40.

[31] S. Silver, Bacterial silver resistance. molecular biology and uses and misuses of silver compounds, FEMS Microbiol. Rev. 27 (2003) 341–353.

[32] S.L. Percival, P.G. Bowler, D. Russell, Bacterial resistance to silver in wound care, J. Hosp. Infect. 60 (2005) 1–7.

[33] W. Wang, P.S. Rainbow, Influence of metal exposure history on trace metal uptake and accumulation by marine invertebrates, Ecotox. Environ. Saf. 61 (2005) 145–159.

[34] S. Franke, G. Grass, D.H. Nies, The product of the ybdE gene of the Escherichia coli chromosome is involved in detoxification of silver ions, Microbiology 147 (2001) 965–972.

[35] S. Franke, G. Grass, C. Rensing, D.H. Nies, Molecular analysis of the copper-transporting efflux system CusCFBA of Escherichia coli, J. Bacteriol. 185 (2003) 3804–3812.

[36] K.B. Holt, A.J. Bard, Interaction of silver (I) ions with the respiratory chain of Escherichia coli: an electrochemical and scanning electrochemical microscopy study of the antimicrobial mechanism of micromolar Ag^+, Biochemistry 44 (2005) 13214–13223.

[37] D. Zhan, X. Li, W. Zhan, F.-R.F. Fan, A.J. Bard, Scanning electrochemical microscopy: the application of a micropipette-supported ITIES tip to detect Ag^+ and study its effect on fibroblast cells, Anal. Chem. 79 (2007) 5225–5231.

[38] E. Hidalgo, C. Dominguez, Study of cytotoxicity mechanisms of silver nitrate in human dermal fibroblasts, Toxicol. Lett. 98 (1998) 169–179.

[39] K. Poon, M.V. Mirkin, A. Burd, In vitro cytotoxity of silver: implication for clinical wound care, Burns 30 (2004) 140–147.

[40] (a) K.R. Wehmeyer, R.M. Wightman, Cyclic voltammetry and anodic stripping voltammetry with mercury ultramicroelectrodes, Anal. Chem. 57 (1985) 1989–1993;
(b) J. Mauzeroll, J.A. Hueske, A.J. Bard, Scanning electrochemical microscopy. 48. Hg/Pt hemispherical ultramicroelectrodes: fabrication and characterization, Anal. Chem. 75 (2003) 3880–3889.

[41] C.G. Zoski, J.C. Aguilar, A.J. Bard, Scanning electrochemical microscopy: shielding effects on reversible and quasireversible reactions, Anal. Chem 75 (2003) 2959–2966;
(b) W. Miao, Z. Ding, A.J. Bard, Solution viscosity effects on the heterogeneous electron transfer kinetics of ferrocenemethanol in dimethyl sulfoxide−water mixtures, J. Phys. Chem. B 106 (2002) 1392.